Spectrum of Engineering Sciences
ISSN (e) 3007-3138 (p) 3007-312X Volume 4, Issue 5, 2026

ASSESSING THE IMPACT OF WATERSHED MANAGEMENT ON FLOOD DYNAMICS UNDER CLIMATE CHANGE IN THE SWAT VALLEY, KP, PAKISTAN

Muhammad Shehryar Suleman[*1], Dr. Rasheed Ahmed[2], Muhammad Jahangir[3]

[*1]*Masters in Climate Change, University of Haripur, Pakistan*
[2]*Assistant Professor, Department of Soil and Climate Sciences, University of Haripur, Pakistan*
[3]*Department of Soil and Climate Sciences, University of Haripur, Pakistan*

[*1]shehryarkhan0788@gmail.com, [2]rasheedahmad@uoh.edu.pk, [3]jahangir1@uoh.edu.pk

DOI: https://doi.org/10.5281/zenodo.20063737

Keywords
HEC-HMS (Hydrologic Modeling System), HEC-RAS (Hydrologic Engineering Center's River Analysis System), RCP 4.5, RCP 8.5.

Article History
Received: 12 March 2026
Accepted: 22 April 2026
Published: 07 May 2026

Corresponding Author: *
Muhammad Shehryar Suleman

Abstract

Frequent flooding in the Swat River basin, draining the hilly terrain of Hindukush Mountains in the Northern Pakistan, has been intensifying due to rapid urbanization, inadequate flood planning, and climate change particularly in the monsoon season. This study addressed the need to assess future flood hazards and evaluated mitigation strategies for the basin. The research aimed to quantify peak river discharge in different scenarios obtained from the recorded precipitation data and future modeled based scenarios data to explore the flooding characteristics (height and discharge) in the River Swat thematic layer (DEM plus Satellite Image) geometry at the most vulnerable zones of river reaches. A coupled modeling approach integrated HEC-HMS for rainfall–runoff simulation and HEC-RAS for river routing and floodplain inundation. Historical simulations used observed precipitation and derived intensity–duration–frequency (IDF) curves, while future flows were estimated using down scaled climate projections for RCP4.5 and RCP8.5 for years 2032, 2042, 2052, 2062, and 2072 respectively. Results indicated that the historical design flood discharge was approximately 1168.8 m³/s at the basin outlet. Under RCP4.5, projected peak flows increased moderately, whereas under RCP8.5, flood magnitudes increased up to 1441.3 m³/s by 2072. Mitigation simulations revealed that an upstream reservoirs of area 57,507,700 sq meters could effectively attenuate peak flows up to 40.92%. while levee embankments up to 7 meters restrict the discharge within river floodplain and alleviate the flood risk. Combined application of both levees and reservoirs in catchment provided the greatest reduction 39.6% in flood extent. This study highlighted climate change predictions in storm events for the future and ultimate its alliance with River Swat peak flow rates to assess the present river geometry and levees application for flooding conditions which can support policy makers to assess the significance of different flood alleviation measures in the Swat Valley and similar regions in South Asia.

Spectrum of Engineering Sciences
ISSN (e) 3007-3138 (p) 3007-312X Volume 4, Issue 5, 2026

GRAPHICAL ABSTARCT

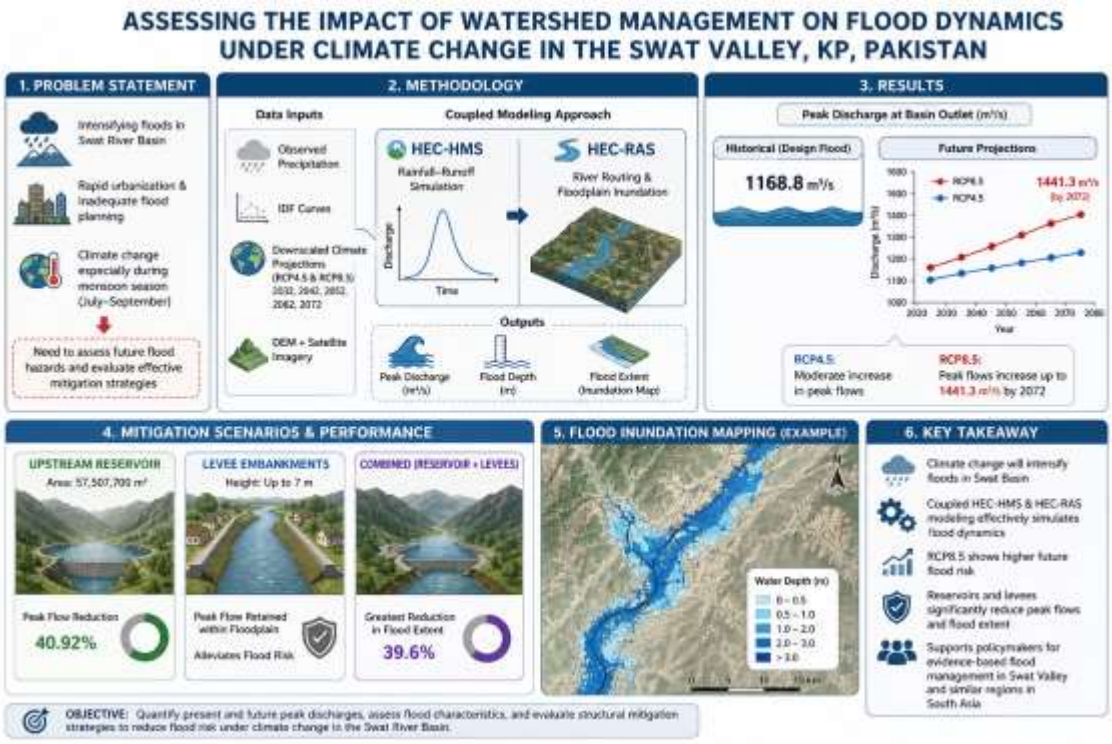

1. INTRODUCTION

In Pakistan's Khyber Pakhtunkhwa (KP) province, the Swat Valley has been more vulnerable to extreme floods. Significant hydrological issues results from these floods, which are mostly caused by erratic cloudbursts and rapid snowmelt during the late monsoon season (July to September). In addition to causing immediate flooding, the heavy rains also exacerbate secondary risks including mudslides, landslides, soil erosion, and sediment deposition downstream. The devastating potential of these floods were further increased by the Swat River's steep grade, which frequently cause significant damage to local communities and infrastructure. Deforestation, change in land use, and poor watershed management are examples of anthropological causes that has exacerbated the Swat Valley's inherent vulnerabilities. When forest cover is lost, the land's ability to absorb rainwater is diminished, which increases surface runoff and the risk of flooding. Urbanization and agricultural expansion into flood-prone areas are examples of land use changes that altered natural water flow patterns and reduced the watershed's ability to withstand severe precipitation. The area still experience regular and severe floods that upended local populations, destroy infrastructure which also limits agricultural production and supply (Ali et al., 2019). The Swat Valley is especially vulnerable to severe flooding because of its steep gradient and extremely unpredictable climate. Rapid melting from the Hindu Kush and Karakoram Mountain ranges, heavy monsoon rains, and erratic cloudbursts are the main natural causes of flood events in the area. Hydro-logically the valley is greatly influenced by the monsoon season, which lasts from July to September. During this time, flash floods and riverine flooding are caused by extreme precipitation, which frequently exceeded 100 mm in a single day. When continuous heavy rainfall and saturated soil conditions coexist, the monsoonal impact is very severe, increasing surface runoff and peak river flow levels. Estimating runoff and understanding the hydrological and hydraulic characteristics of a basin through HEC-RAS and Arc-GIS is considered one of the ideal modelling technique. Non-parametric tests are used to analyze trends in the processed data. Annual peak flows and precipitation totals are subjected to the Mann-Kendall test in order to

identify statistically significant trends at the 5% level (Pal et al., 2023).In HEC-HMS, the semi-distributed rainfall–runoff model was constructed. Using the DEM, the basin was separated into smaller basins or sub basins according to the stream network and terrain. Based on soil and land use, rainfall infiltration was calculated for each sub-basin using the SCS Curve Number loss method. With parameters (lag time, time of concentration) determined by basin geometry and the CN value, the transformed runoff was calculated using a unit hydrograph approach (e.g., Clark unit hydrograph). The lag approach was employed for channel routing (Bentura et al., 1997). HEC-HMS norms were followed in defining the model's basin, meteorological, and control components.HEC-RAS was used to create a 1D/2D hydraulic model of the Swat River channel (Yao et al., 2021). River centerlines, banks, and cross-section profiles were created by utilizing HEC-GeoRAS (ArcGIS) to extract the cross-sectional geometry of the river from the DEM. According to land cover and channel conditions, each channel and floodplain cross-section was given a Manning's roughness (n) value (Milisic et al., 2023). At the upstream end of each river reach, the calibrated flood hydrographs from HEC-HMS were used as the inflow boundary conditions. The water surface elevation and overbank flow along the river were then simulated using HEC-RAS (Horritt et al., 2002).In order to validate the model, historical flood data or high-water marks were compared to simulated inundation (depth and extent) or stage-discharge relationships. Manning's n and channel geometry were adjusted as necessary (Pappenberger et al., 2005). The NASA Earth Exchange Global Daily Downscaled Projections dataset (NEX-GDDP-CMIP6) provided the future climatic precipitation data. To reflect mid- and late-century conditions, we chose time slices that were centered on the years 2032, 2042, 2052, 2062 and 2072. The RCMs' monthly or daily precipitation fields were bias-corrected using change-factor or linear-scaling techniques to reflect modeled changes while maintaining the observed climatology.Peak discharge hydrographs were generated by the calibrated HEC-HMS model for both the baseline and future scenarios. To model flood levels and inundation patterns, these were loaded into HEC-RAS. Both nature-based and structural flood mitigation strategies were modeled and designed in the study.

2. METHODOLOGY

The Swat River flows in a mid of Swat valley and on the south west side it meets with Kabul River near Charsadda (approximately 34.1167° N –71.7167°4 E) latitude and 72°08′53″–72°30′50″ E longitude (Ali et al., 2025). It originates in the high glacial valleys of the Hindu Kush where the Ushu and Gabral meet at Kalam. Steep elevation and land-use gradients in the basin including rocky alpine headwaters, with wider piedmont/plains, influence the runoff route and river morphology. The hydrology is strongly nival-pluvial: the South Asian monsoon particularly in its peaks (July and August) drives seasonal maxima, while spring snowmelt from the Hindu Kush sustains perennial flows. Their interaction, along with the rapid urbanization along floodplains and in valley bottoms, increases the risk of flash floods in a warming climate. Growing hazard with the passage of time, is firstly demonstrated in the recent events such as the 2022 monsoon flooding which affected infra structure and settlements with heavy rainfall and debris-filled overflows. The bench mark to delineate the River Swat basin was selected nearby the Shamozai village which covered an area of 5215 km^2.

2.1 Map of the Study Area

The Swat River Basin, a mountainous to alluvial river system in the eastern Hindu Kush region of northern Pakistan, is the subject of this study. It is distinguished by its steep topography, snowmelt-monsoon hydrology, and dense riparian towns.

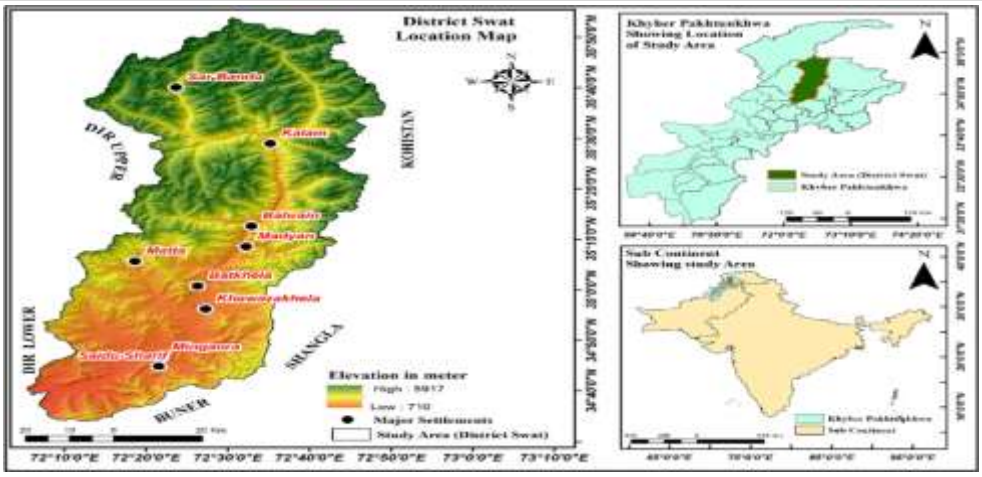

Figure 1 Presenting the Swat River Watershed

2.2 Data Source

A high-resolution Digital Elevation Model (DEM) like Shuttle Radar Topography Mission (SRTM 30 m) and Geographic Information System (GIS) technologies were used to delineate the Swat River basin. Maps of land use and soil were obtained in order to describe hydrologic characteristics. Using ArcGIS, the runoff Curve Number (CN) values for each sub-basin were calculated by superimposing land-use and soil layers.

2.3 In-situ Data

NASA's satellite products provided daily precipitation grids, which were used to collect historical climate data from 2002 to 2022. For use in hydrologic modeling, these were transformed (for example, from Power NASA and Climate engine.org) to provide basin-averaged rainfall time series. For the purpose of calibrating the model, observed streamflow or flood gauge records (where available) were gathered.

The present study employs an integrated hydrological and hydraulic modeling framework to assess current and future flood hazards under climate change scenarios. Initially, spatial and hydro-meteorological data were collected from multiple sources. A 30 m resolution DEM (USGS, UTM 43N, WGS 1984) was used for watershed delineation, river geometry extraction, and slope characterization. Historical rainfall data were obtained from meteorological stations, while supplementary climate data were accessed from the NASA POWER portal. River discharge records were incorporated for calibration and validation of the hydrological model. Trend analysis of historical rainfall and discharge series was conducted using the non-parametric Mann–Kendall test to identify significant changes in precipitation and streamflow behavior over time. For hydrological simulation, the HEC-HMS model was employed.

2.4 Analysis of Trend and Frequency

Non-parametric tests are used to analyze trends in the processed data. Annual peak flows and precipitation totals are subjected to the Mann-Kendall test in order to identify statistically significant trends at the 5% level (Pal et al., 2023). To choose a probability distribution, peaks from at least 10 to 20 years are fitted. Appropriate distributions are found using confidence intervals and goodness-of-fit tests, such as the Chi-squared test. Design flows, such as 50-year or 100-year return periods, are derived from the fitted curve (Ahmed et al., 2025).

In HEC-HMS, the semi-distributed rainfall–runoff model was constructed. Using the DEM, the basin was separated into smaller basins or sub basins according to the stream network and terrain (Ismael et al., 2017). Based on soil and land use, rainfall infiltration was calculated for each sub-basin using the SCS Curve Number loss method. With parameters (lag time, time of concentration) determined by basin geometry and the CN value, the transformed runoff was calculated using a unit hydrograph approach (e.g., Clark unit hydrograph) (Green et al.,

2022). The lag approach was employed for channel routing (Bentura et al., 1997).
HEC-RAS was used to create a 1D/2D hydraulic model of the Swat River channel . River centerlines, banks, and cross-section profiles were created by utilizing HEC-GeoRAS (ArcGIS) to extract the cross-sectional geometry of the river from the DEM.

2.5 Simulation of Flood

Peak discharge hydrographs were generated by the calibrated HEC-HMS model for both the baseline and future scenarios. To model flood levels and inundation patterns, these were loaded into HEC-RAS. We looked at how higher peaks and larger flood extents will result from increased rainfall intensity and volume in future scenarios. Unless modified to account for changes in land use, time-of-concentration, CN, and other characteristics remained constant.

3. RESULTS AND DISCUSSION

3.1 Trend Analysis of Rain Fall

The Mann-Kendall trend analysis of annual rainfall from 2002 to 2022. Although interannual variability is evident, the Sen's slope line indicates a statistically increasing trend in rainfall over the study period. Notable peak rainfall events occurred in 2010 and 2022, while years like 2004 and 2009 recorded comparatively lower values. Overall, the trend suggests a gradual increase in annual rainfall, despite fluctuations in individual years.

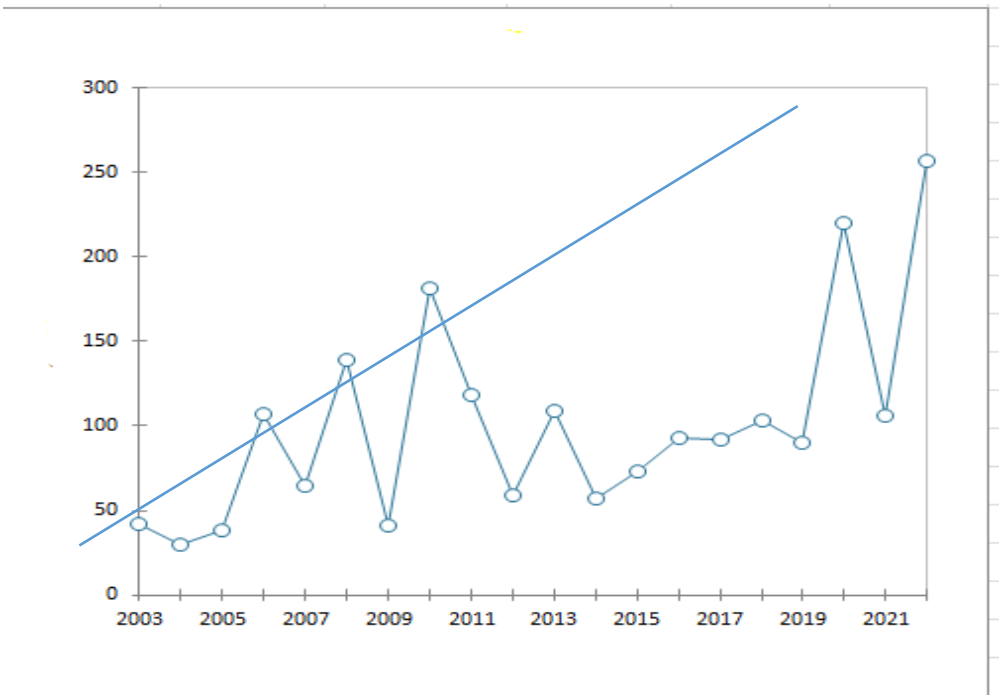

Figure 3.1 Significant increasing trend in annual rainfall detected by Mann-Kendall test (2002–2022)

3.2 Intensity-Duration-Frequency (IDF) Analysis

The IDF curves was developed using historical rainfall data illustrate a clear inverse relationship between rainfall intensity and storm duration across various return periods (2, 10, 25, 50, 75, and 100 years). As the duration increases, rainfall intensity decreases for all return periods, consistent with typical hydrological patterns. Notably, the 100-year return period exhibited the highest rainfall intensity (40.00 cm/hr for a 1 hour event), indicating a significant risk of extreme short-duration storms. These curves provide essential input for hydrologic modeling and the design of flood mitigation infrastructure in the Swat River basin.

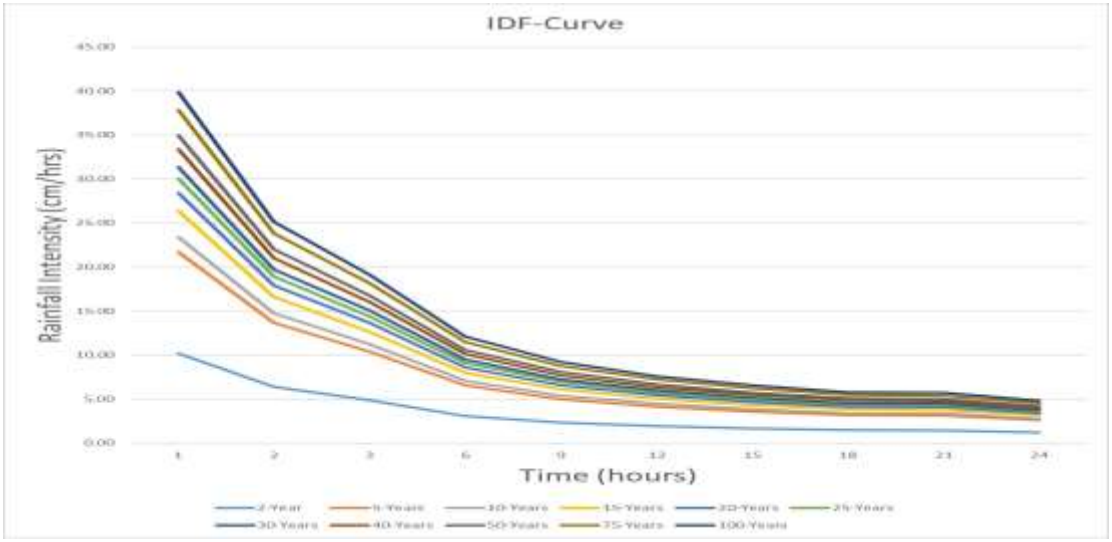

Figure 3.2 Intensity-Duration-Frequency (IDF) Curves for Swat River Basin based on historical rainfall data for 2-, 10-, 25-, 50-, 75-, and 100-year return periods

3.3 Hydrological Modeling of River Swat Basin

The terrain processing technique was applied in HEC-HMS 4.12, to provide direct hydrologic modeling based on Digital Elevation Model (DEM) inputs which were defining the watershed of the Swat River. Key topographic features, such as flow direction, stream network, and watershed borders, were automatically retrieved from a 15-meter resolution SRTM DEM using HEC-HMS's built-in GIS capabilities as illustrated in figure 3.3.

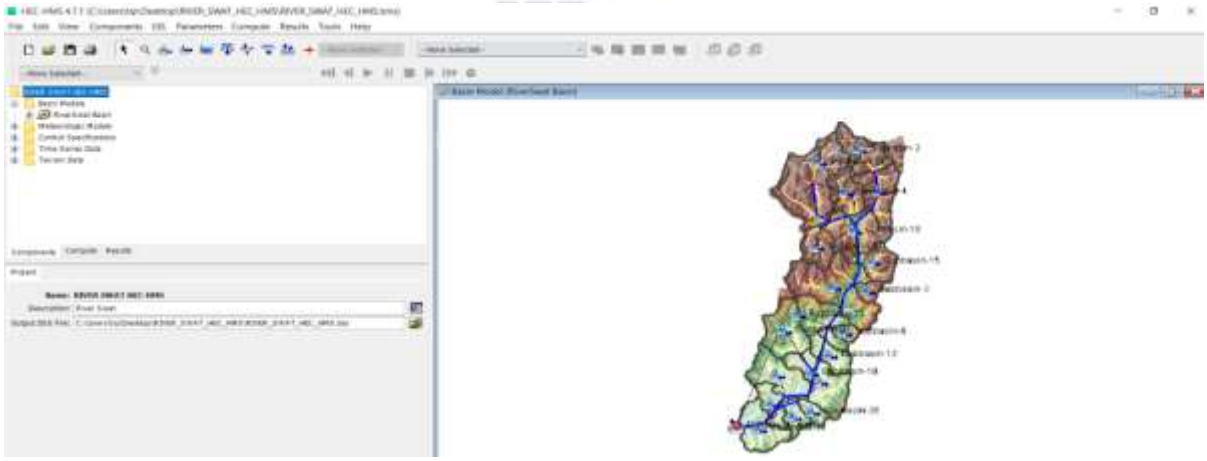

Figure 3.3 DEM-based Watershed Delineation and Stream Network Generated in HEC-HMS.

Using the delineated teerain, the basin model was constructed with 37 sub-basins, each defined according to slope, drainage area and stream connectivity. Hydrologic parameters, including land use, soil type, ans SCS Curve Number (CN), were asssigned manually witin HEC-HMS using reference tables and guidelines.

To run the model, daily rainfall data from 2002 to 2022 were obtained from NASA's GPM and TRMM satellite products. These were downloaded and converted to time series inputs, and processed to calculate basin average precipitation, which was imported as gage data into HEC-HMS.

3.4 Observed vs Simulated Stream flow

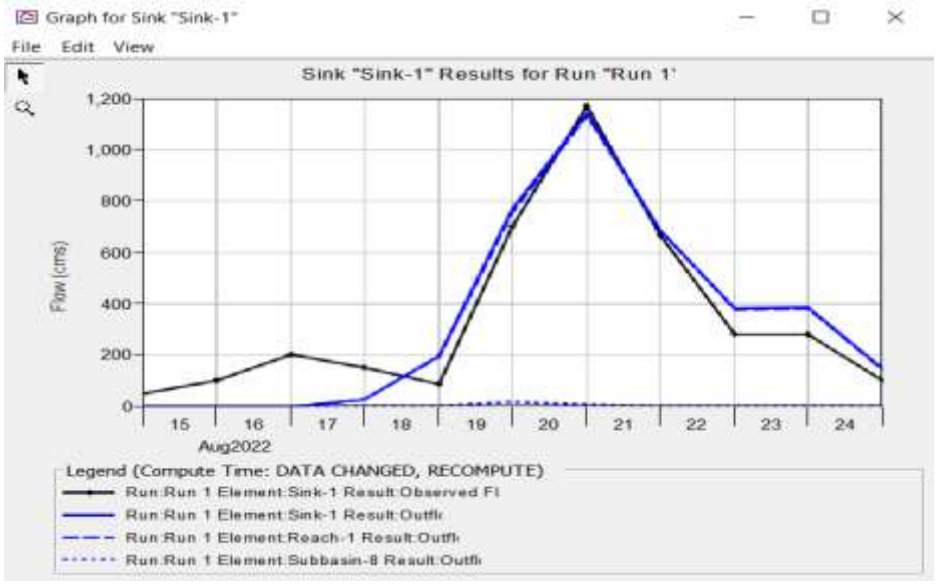

Figure 3.4 Observed vs Simulated Streamflow comparison of Historical Storm Event (HEC-HMS Output)

Model callibration was performed using observed streamflow data from various meteorological stations While there is no single, officially designated meteorological station specifically named "Swat" by the Pakistan Meteorological Department, there are stations and forecast data available for the Swat region, including locations like Swat Ranizai, and data is collected across various locations in the Swat River Basin for scientific study. Weather information is accessible through national meteorological services and commercial weather websites.

The following values were calculated for the basins as;

- Root Mean Square Error (RMSE Std Dev): 0.2
- Percent Bias (PBIAS): 0.97%
- Nash–Sutcliffe Efficiency (NSE): 0.91

These values indicated excellent model performance, as NSE > 0.90 is generally considered highly reliable in rainfall-runoff simulations

3.5 Climate Change Scenarios

To assess the impact of climate change on flood behavior in the Swat River, rainfall projections were input into the calibrated HEC-HMS model for the year 2022 to simulate peak discharges. Hydrographs in Figures 3.5, 3.6, 3.7, 3.8, 3.9, 3.10, 3.11, 3.12, 3.13 and 3.14 show higher peaks under RCP8.5 than RCP4.5, especially in 2072, indicating greater flood risk under severe climate change.

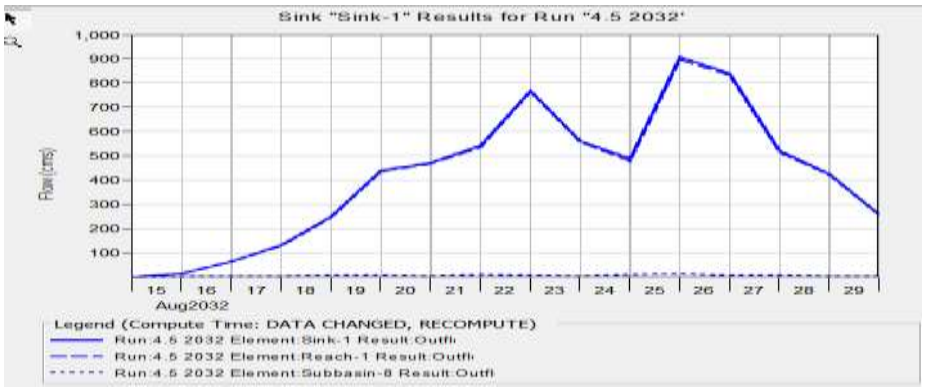

Figure 3.5 Modeled Storm Event under RCP 4.5 (2032 Scenario) HEC-HMS Output

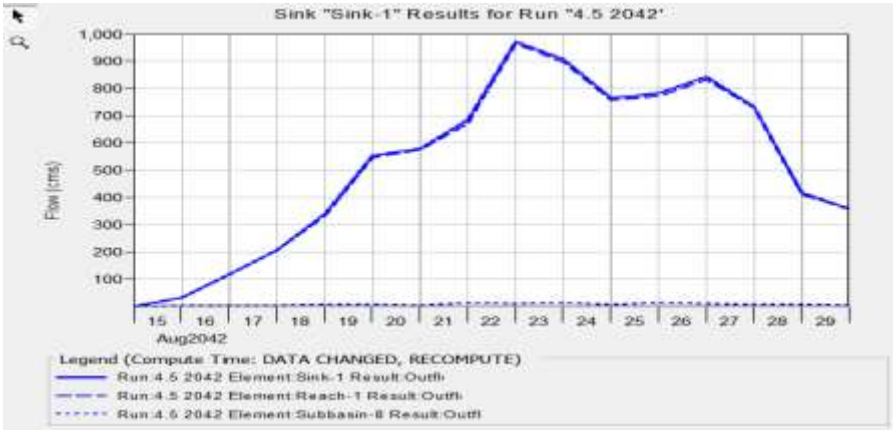

Figure 3.6 Modeled Storm Event under RCP 4.5 (2042 Scenario) HEC-HMS Output)

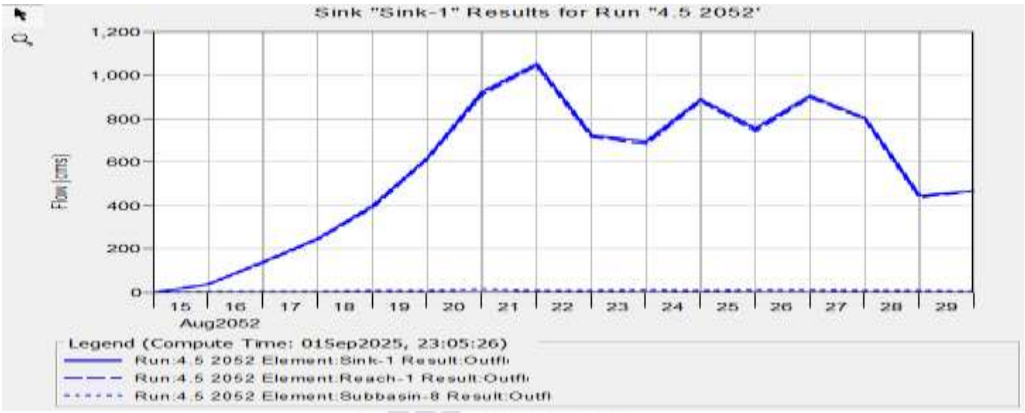

Figure 3.7 Modeled Storm Event under RCP 4.5 (2052 Scenario) HEC-HMS Output.

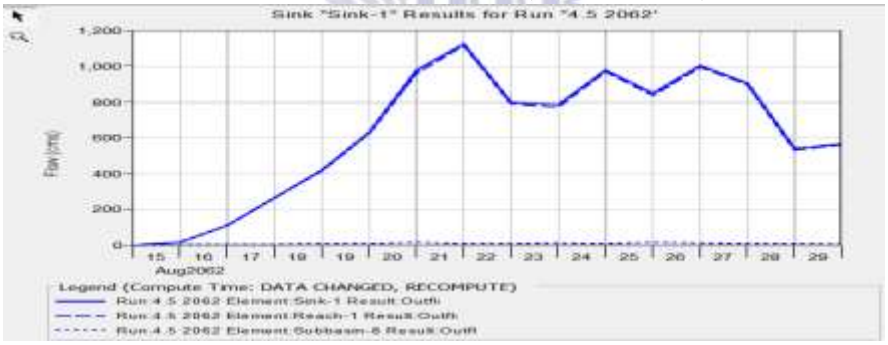

Figure 3.8 Modeled Storm Event under RCP 4.5 (2062 Scenario) HEC-HMS Output

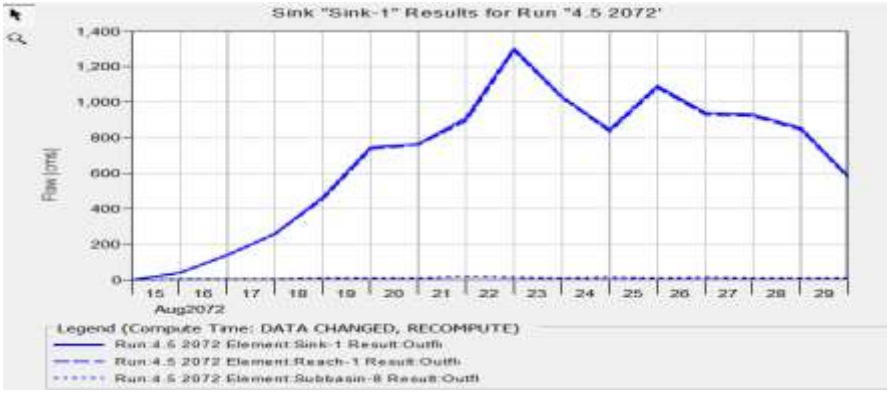

Figure 3.9 Modeled Storm Event under RCP 4.5 (2072 Scenario) HEC-HMS Output

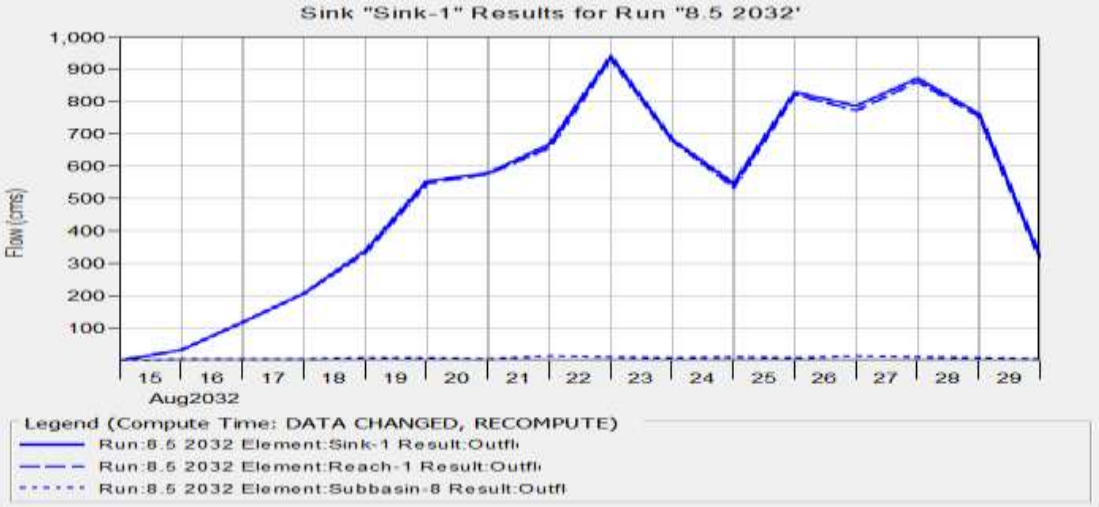

Figure 3.10 Modeled Storm Event under RCP 8.5 (2032 Scenario) HEC-HMS Output

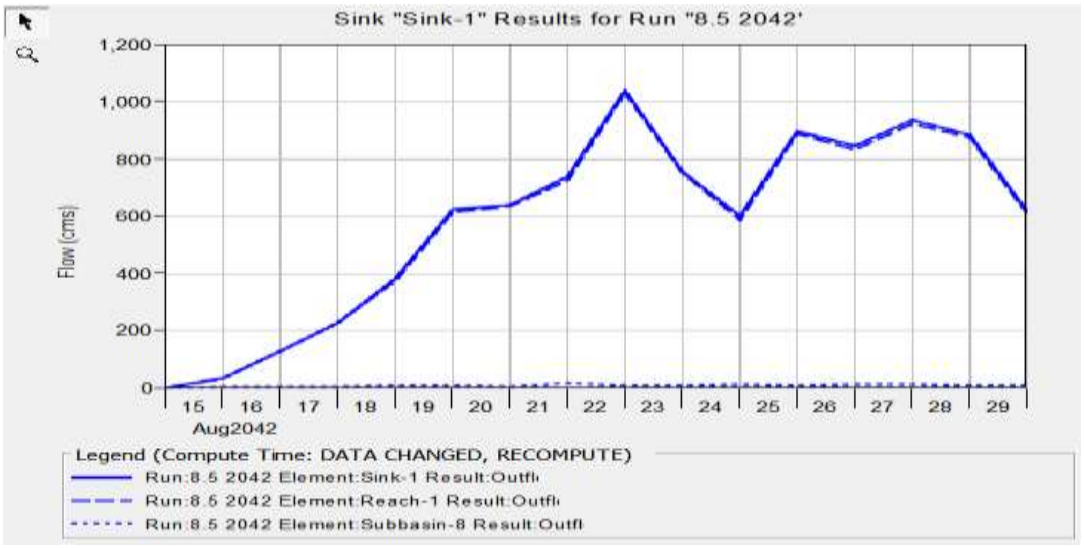

Figure 3.11 Modeled Storm Event under RCP 8.5 (2042 Scenario) HEC-HMS Output

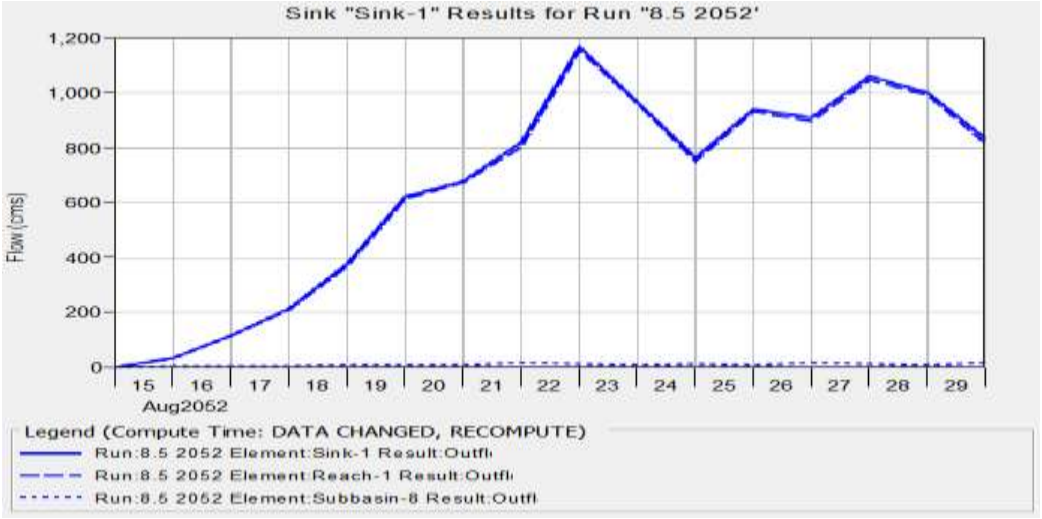

Figure 3.12 Modeled Storm Event under RCP 8.5 (2052 Scenario) HEC-HMS Output

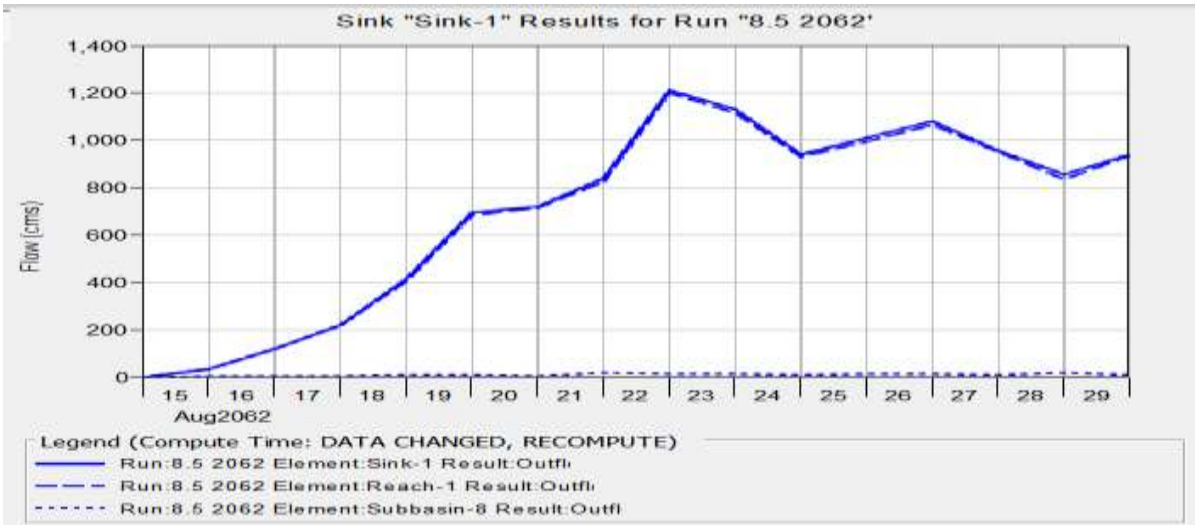

Figure 3.13 Modeled Storm Event under RCP 8.5 (2062 Scenario) HEC-HMS Output

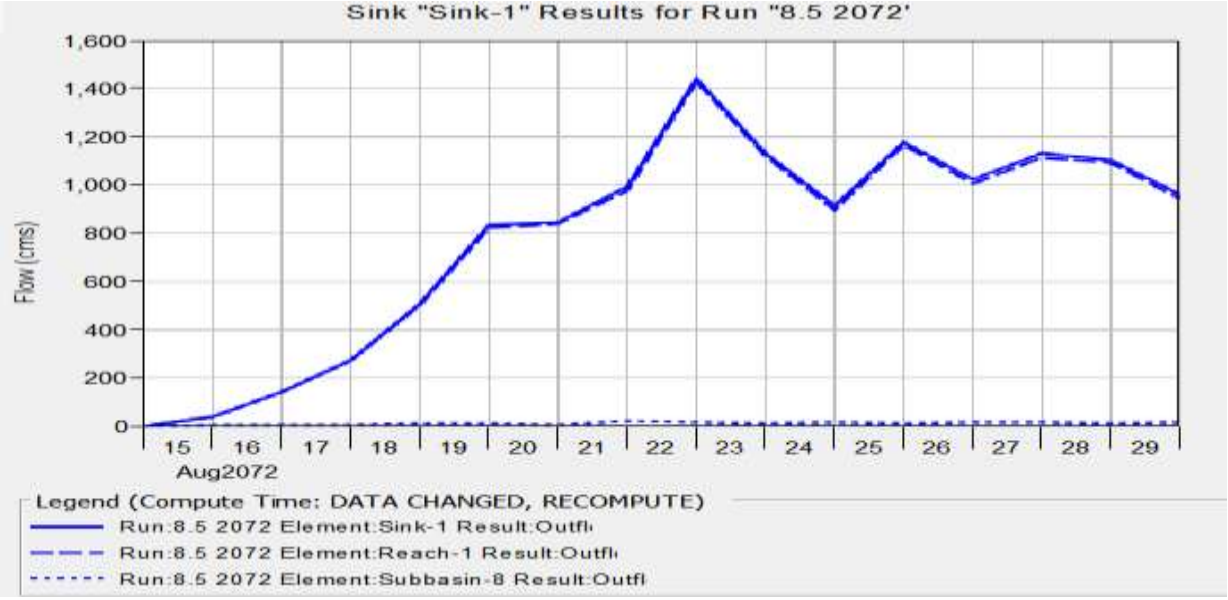

Figure 3.14 Modeled Storm Event under RCP 8.5 (2072 Scenario) HEC-HMS Output

3.5.1 Interpretation

Under RCP4.5, peak discharges raised from 908 m^3/s (2032) to 1302.7 m^3/s (2072), indicating moderate increase is observed in flow rates and then, Under RCP8.5, this increased was observed from 940.4 m^3/s (2032) to 1441.3 m^3/s (2072), showing an inclined increase in flood risk as shown in figure 3.15 and this increment in flow will have to go for the mitigation strategies underscoring the need for adaptive management in the Swat River basin. Rate indicates the need of adaptive management to control flooding in Swat Valley. These findings highlight the necessity of infrastructure and urban planning for the sack of climate resilience.

Figure 3.15 Projected Swat River discharge (m³/s) under RCP 4.5 and RCP 8.5 for 2032, 2042, and 2052,2062,2072.

3.5.2 HEC-RAS 2D Model to Analyze Flood Inundation Mapping Historical and projected peak discharge values

By using HEC-RAS 2D Model it was Analyzed Flood Inundation Mapping Historical and projected peak discharge values from HEC-HMS simulations and climate forecasts under RCP4.5 and RCP8.5 and were utilized as input for the unsteady 2D flow simulation in HEC-RAS in order to model the flood behavior of the Swat River. To ensure consistency with actual flood behavior, the model was calibrated using historical discharge records (2002–2022) and verified against observed peak stages. After a successful calibration, flood scenarios based on peak discharges for 2032, 2042, 2052, 2062 and 2072 were simulated. The time-series flood extents and maximum inundation depths generated by each simulation were post-processed in RAS Mapper. To pinpoint vulnerable areas during certain periods of important peak flows, flood maps were created as given in figure 3.16.

3.6 Effectiveness of Natural and Constructed Techniques

3.6.1 Flood-Prone Areas and Levee Design

The hydraulic simulation identified station 12306, 13902 and station 22395 as highly flood-prone locations along the Swat River. Levee constructions were tested against peak flow rate at these sites as shown in figure 3.16, 3.17 and 3.18 to reduce the risk of flooding:

- Station 12306: A levee of 4 m height was constructed on the left bank, while a 5 m levee was designed on the right bank.
- Station 13902: A levee of 6 m height was designed on the left bank, and a 7 m levee on the right bank, providing adequate protection against projected peak flows.
- Station 22395: A levee of 5 m height was constructed on the left bank, while a 8 m levee was designed on the right bank.

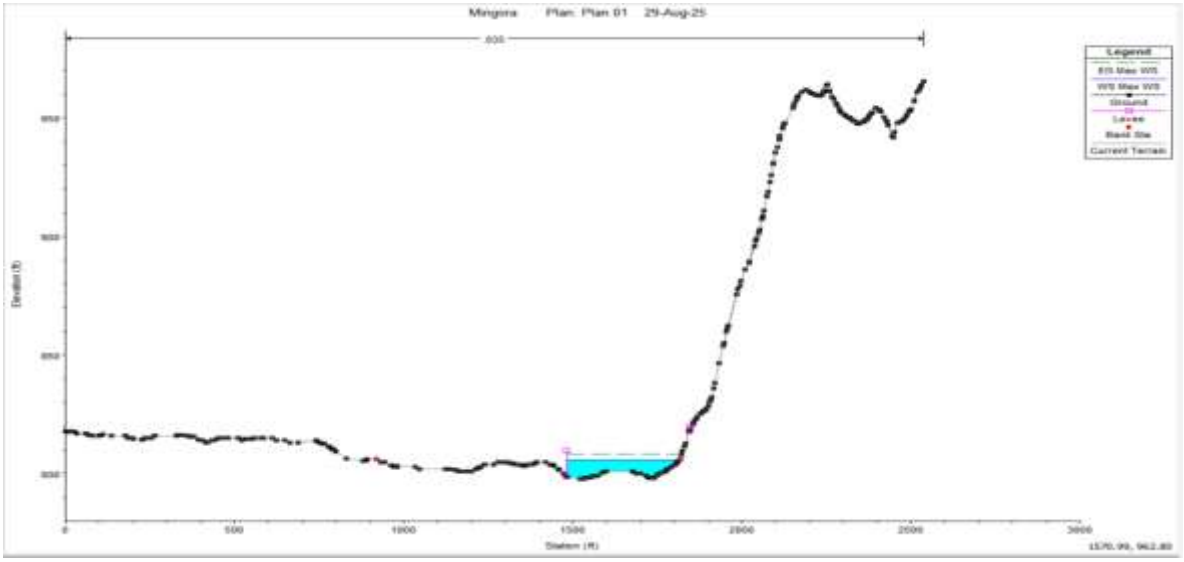

Figure 3.16 Levee application at River station 12306

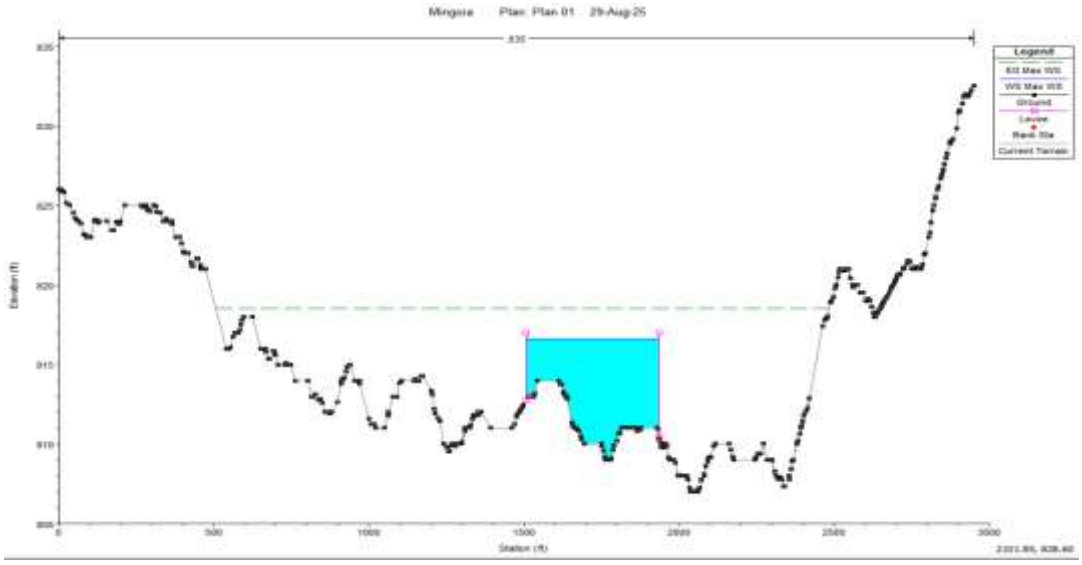

Figure 3.17 Levee application at River station 13902

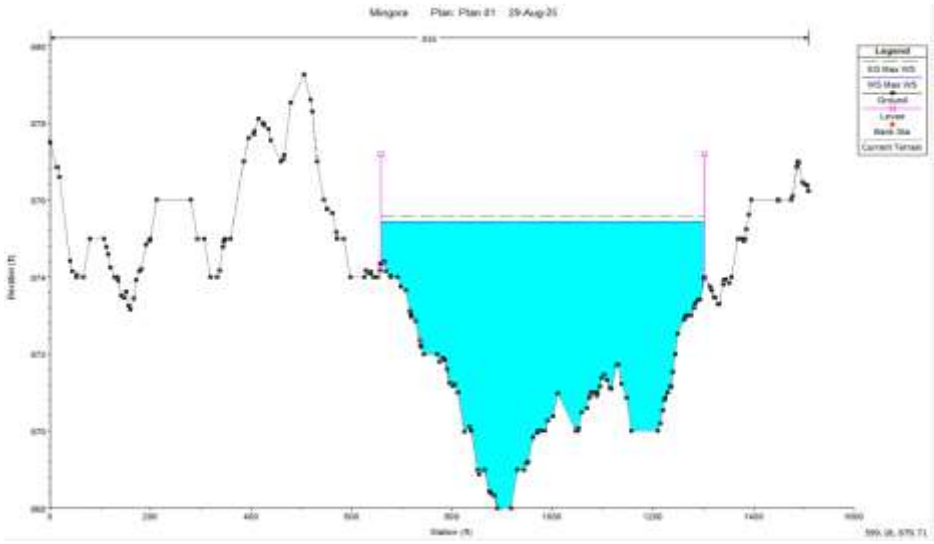

Figure 3.18 Levee application at River station 22395

3.7 Impact of Levee Application

The modeling results showed a significant decrease in inundation following the installation of levees on the designated flood-prone locations, as shown in Figure 3.19. Under design discharge circumstances, the protected zones demonstrate flow confinement inside the riverbanks, lowering the risk of flooding in nearby communities and agricultural areas.

Figure 3.19 Post levee application flood extent, indicating reduced inundation in lood-prone areas

3.8 Stage Discharge Relationships for Swat River Stations

3.8.1 RS12306 Rating Curve

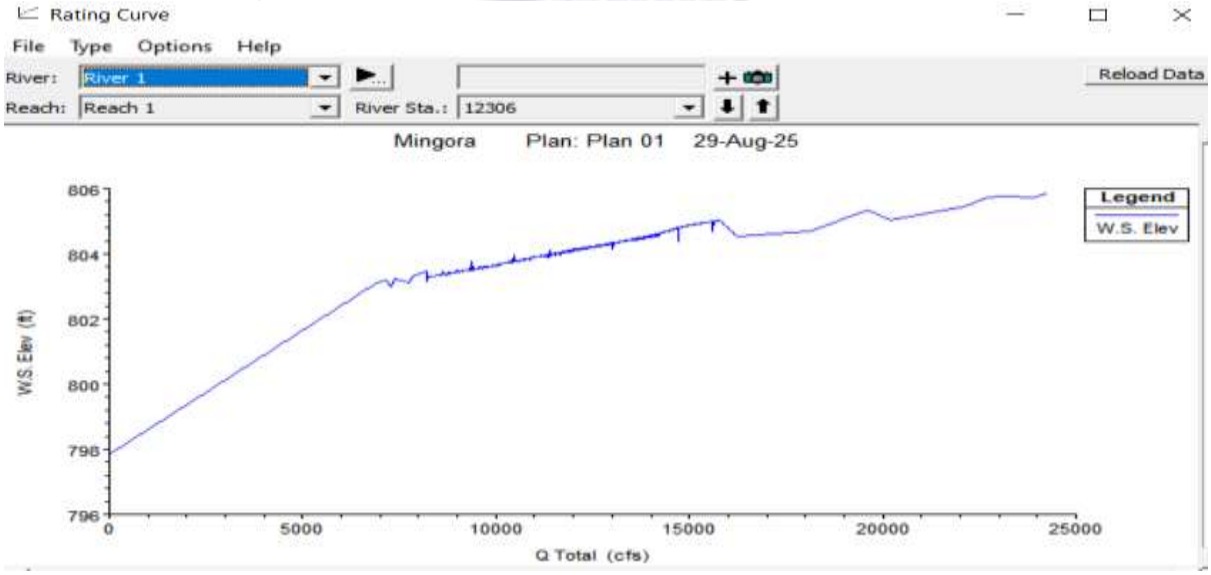

Figure 3.20 Rating curve for RS12306, Swat River (stage–discharge relationship with levee heights)

At station RS12306, the stage discharge relationship was derived using a power-law fit, resulting in the equation Q = 1.23H^1.87, where Q is discharge (m^3/s) and H is stage (m). The model performance was satisfactory, with an R^2 value of 0.95 and an RMSE of 2.3 m^3/s. The water surface elevation (WSE) line, denoted as W_s, remained consistently below the levee heights (4.0 m on the left bank and 5.0 m on the right bank), demonstrating that the river channel at this location has sufficient

capacity to contain the measured flows. Figure 3.20 presents the rating curve for RS12306.

3.8.2 RS13902 Rating Curve

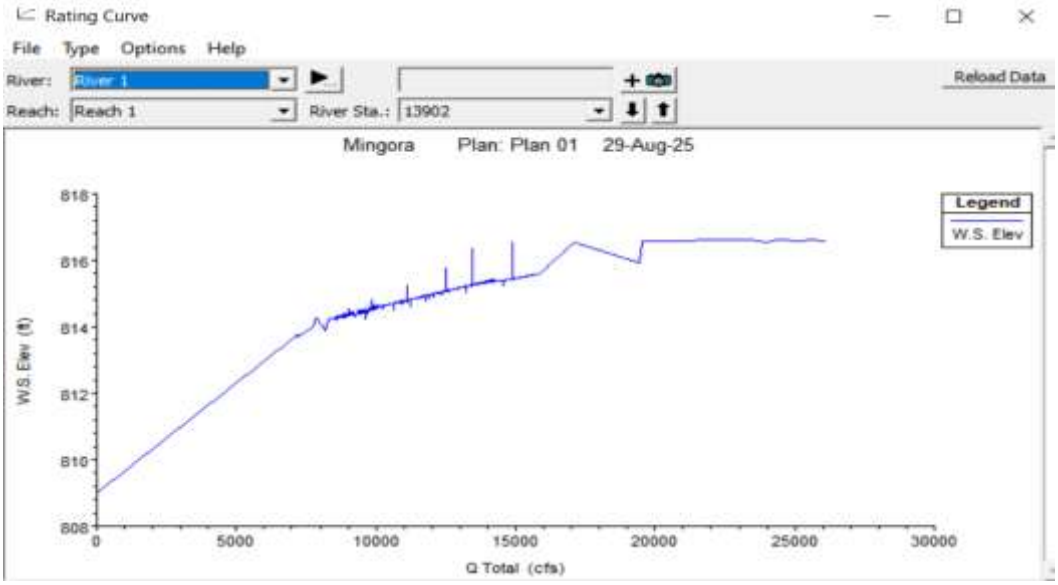

Figure 3.21 Rating curve for RS13902, Swat River (stage–discharge relationship with levee heights).

For station RS13902, the fitted stage discharge relationship followed the equation $Q = 1.50H^{2.05}$, with Q in m³/s and H in meters. The relationship achieved a strong statistical fit, with an R^2 value of 0.97 and an RMSE of 1.8 m³/s, indicating high accuracy in representing the observed data. The WSE line remained below the levee heights (6.0 m on the left bank and 7.0 m on the right bank), confirming sufficient flood protection capacity at this station. Figure 3.21 illustrates the rating curve for RS13902.

3.9 Simulated Reservoir for Flood Management

A total of 15 potential reservoir sites were identified and digitized along different locations of the Swat River using Google Earth imagery and GIS tools. These sites were selected based on topographic suitability and available storage capacity.

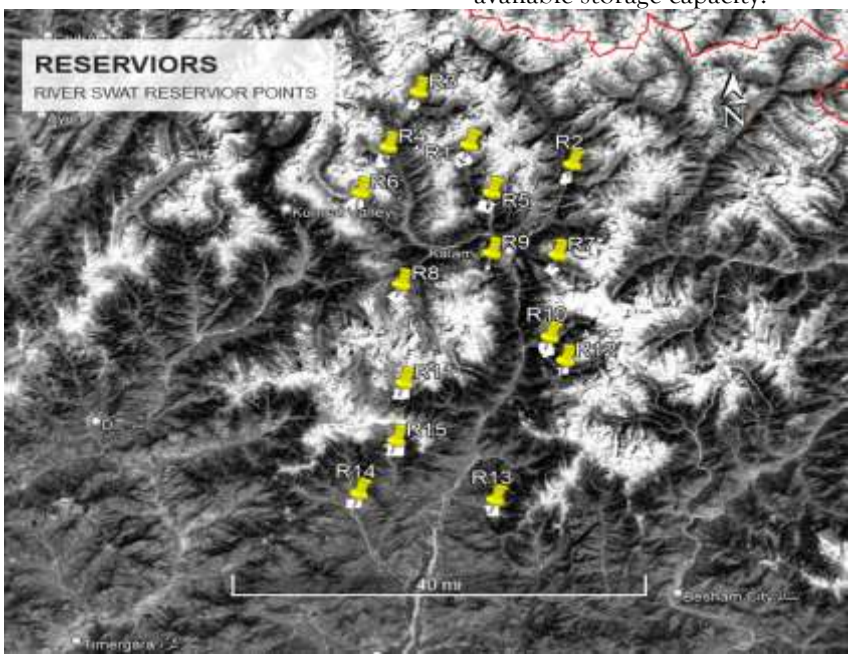

Figure 3.22 Potential locations of 15 reservoirs identified along the Swat River using Google Earth imagery and GIS analysis

3.10 Cumulative Outflow

The results show that the cumulative outflow before reservior application was 281120.7× 10^3 m^3 which decreased to 166105.3 × 10^3 m^3 after incorporating the reservoir,This corresponds to a reduction of about 115015.4× 10^3 m^3. that is about 40.92%.

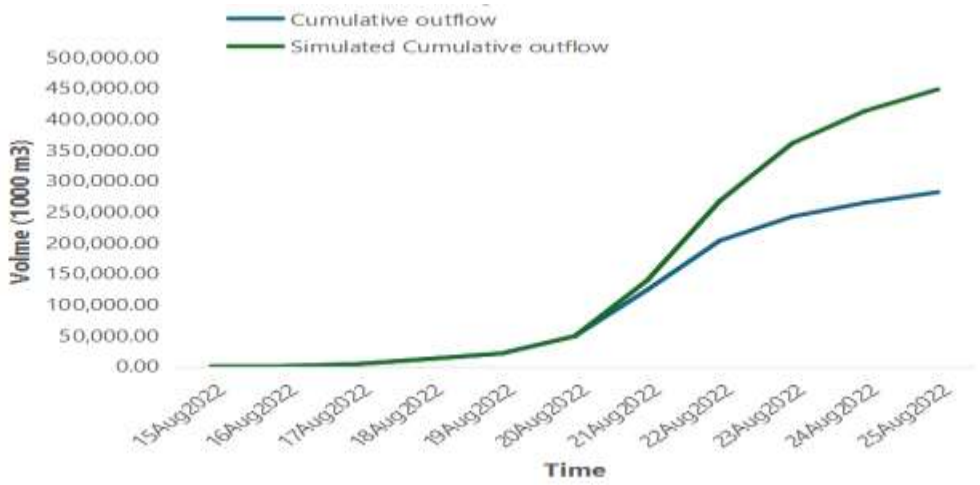

Figure 3.23 Cumulative outflow before and after reservoir implementation.

3.10.1 Effect of Reservoirs on Peak Flow

The peak inflow before applying reservoirs was 1168.0 m^3/s, while after the simulation with reservoir-based flood management, the peak inflow was reduced to 771.9 m^3/s. This shows a reduction of about 396.1 m^3/s (≈39.6%), indicating the effectiveness of reservoirs in lowering peak flood discharge.

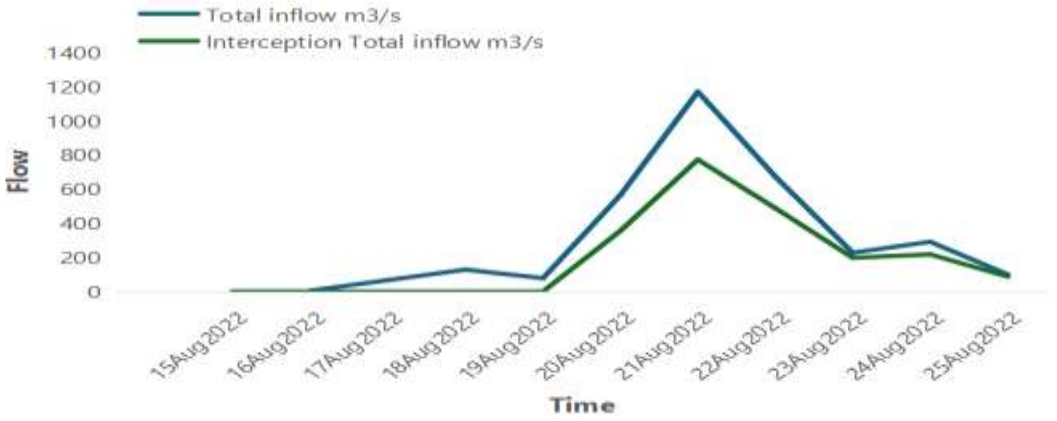

Figure 3.24 Comparison of inflow hydrograph before and after reservoir implementation

The analysis of historical rainfall and streamflow highlights the increasing hydrological variability in the Swat River Basin. The Mann–Kendall test confirmed a rising trend in precipitation from 2002–2022, consistent with observed regional shifts in South Asian monsoon patterns. The IDF analysis further underscored the risk of short-duration, high-intensity rainfall, with extreme events such as the 100-year, daily storm exceeding 40.00 cm/hour. Such rainfall magnitudes are critical in semi-arid catchments where infiltration capacity is limited, resulting in rapid runoff and flash flooding. These findings align with studies demonstrating that IDF relationships are vital for understanding rainfall extremes and their impact on urban hydrology (Wu et al., 2022). The hydrological modeling performed using HEC-HMS produced reliable results, with calibration statistics (NSE = 0.91, PBIAS = 0.97%) indicating excellent agreement between simulated and observed flows.

Under projected climate change scenarios, peak discharges increase significantly, particularly under RCP8.5. While RCP4.5 scenarios

showed a moderate rise from 908 m³/s in 2032 to 1302.7 m³/s in 2072, RCP8.5 values rose more sharply from 940.4 m³/s to 1441.3 m³/s in the same period that is (2032-2072). These results align with regional climate assessments which show that RCP8.5 pathways typically produce more severe hydrological extremes compared to RCP4.5. The implication is that unless emissions are reduced globally, the Swat River Basin could face flood magnitudes nearly double those of the historical record by the end of the century.

4. CONCLUSION

This study demonstrates that the Swat River Basin is highly vulnerable to increasing flood risks under changing climatic conditions. Historical analysis confirmed rising rainfall trends and produced a calibrated peak discharge of 1168.8 m³/s, with strong model performance validating its reliability. Future projections showed moderate increases under RCP4.5 and much larger rises under RCP8.5, with peak flows increasing historical values by 2072. These results confirm that climate change will significantly intensify flood magnitudes, especially under high-emission conditions. Flood inundation mapping further highlighted the vulnerability of low-lying and urban-adjacent areas, where inundation depths may reach several meters in future scenarios. The simulation of flood mitigation techniques revealed that reservoirs, functioning as nature-based solutions, effectively reduced peak discharges by increasing infiltration, enhancing groundwater recharge, and delaying the time of concentration. Constructed levees, in contrast, acted as engineered barriers that restricted the lateral spread of floods and reduced their penetration into adjacent urban and agricultural areas. The findings suggest that the most effective approach lies in combining these two strategies, where reservoirs reduce overall runoff and peak magnitudes, while levees safeguard vulnerable areas. Overall, the results emphasize the urgent need to align urban planning, infrastructure development, and adaptive measures with projected climate scenarios to achieve long-term resilience in the Swat River Basin.

4.1 RECOMMENDATIONS

Policy and Planning

- Enforce strict land-use zoning to prevent urban development in flood-prone areas.
- Incorporate flood hazard maps and climate projections into urban and regional planning frameworks.
- Designate floodplains as multifunctional spaces such as green belts, parks, or agricultural zones that can safely accommodate floodwaters.

Engineering Measures

- Construct and maintain detention reservoirs and retention basins upstream to regulate peak discharges.
- Upgrade levees, embankments, and other flood protection structures to withstand projected higher flows.
- Enhance urban drainage systems to manage intense short-duration rainfall events.

Nature-Based Solutions

- Restore wetlands, riparian buffers, and reforest upland areas to increase infiltration and reduce runoff.
- We should also promote tree outside forests realizing that the country has a huge potential for increasing its Trees Outside Forest area primarily through expansion of agroforestry, optimum use of waste and barren land.
- Promote soil conservation and sustainable farming practices to improve watershed resilience.
- Encourage ecological floodplain management to balance ecosystem health with flood risk reduction.

Climate Adaptation and Preparedness

- Revise design standards for infrastructure using projected peak discharges instead of historical records.
- Establish early warning and real-time monitoring systems for rainfall and river flow.
- Strengthen community awareness, education, and preparedness programs to build local resilience against flood.
- Avoid false solutions like biofuels, biomass, or carbon offsets that rely on wishful

thinking, yet in practice release more greenhouse gas emissions.

4.2 FUTURE PERSPECTIVES

Future research on flood risk management in the Swat River Basin should move beyond conventional hydrological modeling toward a more integrated, systems-level framework that connects climate change, environmental sustainability, food systems, and human health. While this study employed HEC-HMS and HEC-RAS for hydrological and hydraulic simulations, the increasing complexity of climate-driven hazards necessitates interdisciplinary approaches supported by emerging technologies and cross-sectoral insights.

One key direction involves the integration of artificial intelligence (AI) and data-driven modeling into hydrological forecasting systems. Recent advancements demonstrate that AI-based decision-support tools significantly enhance predictive accuracy and adaptive planning across complex systems (Kamal et al., 2026; Naeem et al., 2026). In flood modeling, such approaches can be combined with physically based models to improve real-time forecasting, optimize reservoir operations, and support early warning systems under rapidly changing climatic conditions.

In parallel, climate-induced hydrological variability has direct implications for food security and nutritional systems. Flood events disrupt agricultural production, alter soil quality, and affect food safety, which aligns with broader research on food system resilience and quality assessment (Butt et al., 2024; Ahmed et al., 2024). The development of sustainable and functional food systems, including plant-based innovations and hybrid protein sources, highlights the need to align environmental management with nutritional sustainability (Butt et al., 2025b; Riaz et al., 2026). Moreover, the role of probiotics and functional foods in improving metabolic health under environmental stress conditions further emphasizes the interconnectedness of ecosystem disruptions and human health outcomes (Rashid et al., 2026).

At the molecular and agricultural level, future adaptation strategies may also benefit from advances in biotechnology and genetic engineering. Techniques such as CRISPR-based genome and epigenome editing have shown strong potential in enhancing crop resilience to environmental stressors, including drought and extreme climate variability (Jabeen et al., 2025; Fatima et al., 2026). These innovations can play a critical role in developing climate-resilient agricultural systems within flood-prone regions, thereby reducing vulnerability at the watershed scale.

Additionally, environmental stressors linked to climate change—including contamination, food adulteration, and exposure to heavy metals—pose increasing risks to public health (Riaz et al., 2026). Nutritional interventions, including micronutrient regulation and phytochemical-rich diets, have been shown to influence metabolic and epigenetic responses under such stress conditions (Butt et al., 2026a; Butt et al., 2026b). These findings suggest that flood risk management should be viewed not only as a hydrological challenge but also as a public health priority.

From a clinical and physiological perspective, environmental disruptions can influence long-term human health outcomes, including musculoskeletal stress, metabolic disorders, and disease susceptibility (Mahmood et al., 2026; Khan et al., 2024). Preventive healthcare strategies, including dietary optimization and therapeutic interventions, should therefore be incorporated into broader climate adaptation frameworks. Similarly, advances in clinical treatments and preventive care—such as minimally invasive dental interventions and periodontal risk management—highlight the importance of integrating healthcare resilience into environmental planning (Jabeen et al., 2026a; Jabeen et al., 2026b).

Beyond technical and biomedical dimensions, future research must also address the socio-economic and sustainability aspects of flood risk management. Sustainable watershed management requires not only engineering solutions but also an understanding of social resilience, governance structures, and environmental ethics (Khurshid et al., 2026). The transition toward sustainable development frameworks must incorporate both environmental performance and social equity, particularly in vulnerable regions facing recurrent climate hazards.

Finally, future modeling efforts should incorporate dynamic land-use change, ecosystem services, and nature-based solutions within a unified framework. Combining green infrastructure approaches with engineered interventions—such as reservoirs and levees—can enhance long-term resilience while minimizing ecological disruption. The integration of multi-sectoral data, AI-driven analytics, and climate-resilient agricultural and health systems represents a critical pathway toward holistic flood risk management in the Swat River Basin and similar environments.

5. REFERENCES

Ahmed, A., Rahman, A., Rafi, R. S., Khan, Z., & Mannan, H. (2025). Statistical and Physical Significance of Homogeneous Regions in Regional Flood Frequency Analysis. Water, 17(12), 1799.

Ahmed, N., Saeed, M., Asghar, A., Butt, M. A., Afzaal, M., Saeed, F., Wahab, R., et al. (2024). Utilization of *Lactobacillus rhamnosus* as a probiotic adjunct culture for the development of tempeh. *International Journal of Food Properties, 27*(1), 1279–1289.

Ali, M., Khan, M. S., & Ullah, S. (2025). *Flood risk assessment in the Swat river catchment through GIS-based multi-criteria decision analysis*. Frontiers in Environmental Science, 13, 1567796. https://doi.org/10.3389/fenvs.2025.1567796.

Ali, S., Liu, Y., Ishaq, M., Shah, T., Abdullah, I., & Ilyas, A. (2019). Climate change and its impact on the yield of major food crops: Evidence from Pakistan. Foods, 8(10), 406. https://doi.org/10.3390/foods8100406

Bentura, P. L., & Michel, C. (1997). Flood routing in a wide channel with a quadratic lag-and-route method. *Hydrological Sciences Journal*, *42*(2), 169-189.

Butt, M. A., Ali, M. A., Ishaq, A., Saleem, A., Hayat, S., & Khalil, N. (2026a). The influence of dietary zinc supplementation on the expression of insulin-like growth factor 1 (IGF-1) in adolescent athletes. *Pakistan Journal of Medical & Cardiological Review, 5*(2), 12–19.

Butt, M. A., Ali, M. A., Ishaq, A., Saleem, A., Saeed, S., & Ul Islam, M. (2026b). Phytochemical-rich functional diet regulates epigenetic markers (DNA methylation) associated with obesity and insulin resistance. *Pakistan Journal of Medical & Cardiological Review, 5*(1), 2707–2715.

Butt, M. A., Arshad, M. U., Imran, A., & Afzaal, M. (2025a). Nutritional and biosafety assessment of a novel soy–whey hybrid protein crosslinked by microbial transglutaminase in Sprague Dawley rats. *TPM: Testing, Psychometrics, Methodology in Applied Psychology, 32*(S7), 597–608.

Butt, M. A., Arshad, M. U., Tasleem, S., Imran, A., & Afzaal, M. (2025c). Comparative analysis of chicken and meat analogue patties: Evaluating physicochemical, cooking, textural, microbial, and sensory attributes. *TPM: Testing, Psychometrics, Methodology in Applied Psychology, 32*(S6), 1274–1285.

Butt, M. A., Shahzad, M. H., Tasleem, S., Riaz, R., Ye, X., Khalid, B., Ashraf, M. A., et al. (2025b). Design of a sustainable whey–corn hybrid protein powder for enhanced nutrition, functionality, and environmental stewardship. *Innovative Research in Applied, Biological and Chemical Sciences, 3*(2), 32–51.

Butt, M. A., Shukat, R., Afzaal, M., Saeed, F., Imran, A., Ahmed, A., Islam, F., et al. (2024). Comparative evaluation of the quality and safety attributes of local and branded beef seekh kabab. *Cogent Food & Agriculture, 10*(1), 2360769.

Fatima, A., Jabeen, N., Butt, M. A., Noman, M., Riaz, T., Saeed, S., Saleem, A., & Sohail, Q. (2026). CRISPR-Cas12a mediated epigenome editing of DNA methylation at the DREB1A promoter enhances drought survival rate by ≥35% in *Zea mays* seedlings. *Research Consortium Archive, 4*(2), 1093–1102.

Herbei, M. V., Bădăluță-Minda, C., Popescu, C. A., Horablaga, A., Dragomir, L. O., Popescu, G., ... & Sestras, P. (2024). Rainfall-runoff modeling based on HEC-HMS model: a case study in an area with increased groundwater discharge potential. Frontiers in Water, 6, 1474990.

Horritt, M. S., & Bates, P. D. (2002). Evaluation of 1D and 2D numerical models for predicting river flood inundation. *Journal of hydrology*, *268*(1-4), 87-99.

Ismael, O., Joseph, S., & Patrick, K. H. (2017). HEC-HMS model for runoff simulation in Ruiru reservoir watershed. *American Journal of Engineering Research (AJER)*, *6*(4), 1-7.

Jabeen, N., Shahzadi, M., Taha, M., Shahzadi, N., & Butt, M. A. (2026a). The impact of orthodontic treatment on periodontal health: Gingival recession, bone loss, and patient-specific risk factors. *Research Consortium Archive*, *4*(2), 1198–1213.

Jabeen, N., Shahzadi, M., Taha, M., Shahzadi, N., & Butt, M. A. (2025). CRISPR-Cas mediated genome editing for disease resistance in crops: Advances and challenges. *Pakistan Journal of Medical & Cardiological Review*, *4*(3), 2677–2689.

Jabeen, N., Shahzadi, M., Taha, M., Shahzadi, N., & Butt, M. A. (2026b). Silver diamine fluoride for caries arrest in pediatric and special needs populations: A decade of clinical evidence. *Pakistan Journal of Medical & Cardiological Review*, *5*(2), 693–704.

Kamal, N., Butt, M. A., & Javeid, U. (2026). An empirical study on the effectiveness of artificial intelligence tools in English language acquisition and teaching strategies within an ESG framework. *Social Science Review Archives*, *4*(1), 3562–3568.

Khan Swati, M., Shahzadi, M., Taha, M., Shahzadi, N., & Butt, M. A. (2026). Silver diamine fluoride for caries arrest in pediatric and special needs populations: A decade of clinical evidence. *Pakistan Journal of Medical & Cardiological Review*, *5*(2), 693–704.

Khan, W. A., Inam-ur-Raheem, M., Rasheed, H., Butt, M. A., Saeed, F., Afzaal, M., Ahmed, F., Akram, N., Asghar, A., & Hailu, G. G. (2024). Comparative effect of olive oil and flaxseed oil on drug-induced hepatotoxicity in rats. *Food Science & Nutrition*, *12*(11), 9673–9681.

Khurshid, J., Babar, Z., Ahmed, S., Butt, M. A., Javeid, U., & Khalil, N. (2026). Beyond carbon footprints: Unpacking the social dimensions of sustainability performance in emerging market firms. *Social Science Review Archives*, *4*(1), 3386–3402.

Mahmood, B., Arif, M., Basit, H. M. M., Nadeem, B., Abdullah, A., & Butt, M. A. (2026). Long-term knee joint loading alterations in athletes 5 years post-ACL reconstruction: A comparative gait analysis. *Pakistan Journal of Medical & Cardiological Review*, *5*(2), 310–318.

Makkena, J. (2016). *Modelling the hydrology of watershed by using HEC-HMS* (Doctoral dissertation, Kelappaji College of Agricultural Engineering and Technology, Tavanur).

Milišić, H., & Hadžić, E. (2023, December). Estimation of channel and flood plain roughness using HEC-RAS model: A case study of the Veseočica River, Bosnia and Herzegovina. In *IOP Conference Series: Materials Science and Engineering* (Vol. 1298, No. 1, p. 012031). IOP Publishing.

Naeem, W., Butt, M. A., & Javeid, U. (2026). From entrepreneurship theory to startup execution: A simulation-based benchmark analysis of AI-enhanced venture decision systems in early-stage business performance. *Social Science Review Archives*, *4*(1), 4065–4075.

Pal, L., Saksena, S., Dey, S., Merwade, V., & Ojha, C. S. P. (2023). An integrative framework for assessment of urban flood response to changing climate. *Water Resources Research*, *59*(8), e2023WR034466.

Pappenberger, F., Beven, K., Horritt, M., & Blazkova, S. J. J. O. H. (2005). Uncertainty in the calibration of effective roughness parameters in HEC-RAS using inundation and downstream level observations. *Journal of hydrology*, *302*(1-4), 46-69.

Peker, İ. B., Gülbaz, S., Demir, V., Orhan, O., & Beden, N. (2024). Integration of HEC-RAS and HEC-HMS with GIS in flood modeling and flood hazard mapping. Sustainability, 16(3), 1226.

Rashid, M. S., Gull, Z., Butt, M. A., Hayat, S., Azam, S. E., Saeed, S., Bashir, M. M., et al. (2026). The role of functional probiotic yogurt consumption in medical weight loss: A GLP-1 friendly nutritional approach to metabolic health in UK adults. *Pakistan Journal of Medical & Cardiological Review*, *5*(1), 1623–1632.

Riaz, T., Azhar, A., Xia, Z., Batool, A., Ye, X., Khalid, B., Khan, M. M., et al. (2026). Advances in plant-based functional foods: Emerging trends, nutritional potential, and health implications. *Food Science & Applied Microbiology Reports*, *5*(1), 1–17.

Riaz, T., Khan, M. M., Fatima, H., Ansar, S., Khalid, B., Batool, A., Riaz, R., et al. (2026). Microbiological safety, adulteration, and heavy metal-associated health risks in raw cow and buffalo milk from Punjab, Pakistan. *Food Science & Applied Microbiology Reports*, *5*(1), 18–28.

Yao, A. B., Anoh, K. A., Brou, L. A., Goli, M. W., & Kouassi, L. K. (2021). Simulation of the Hydrodynamic Functioning of the Cavally River Using a Coupled 1D-2D Model in the Ity Area (Zouan-Hounien in Côte d'Ivoire). *Open Journal of Modern Hydrology*, *11*(4), 75-84